

UC Merced

UC Merced Previously Published Works

Title

Epithelial Infection With *Candida albicans* Elicits a Multi-System Response in Planarians

Permalink

<https://escholarship.org/uc/item/47c3w074>

Authors

Maciel, Eli Isael
Arevalo, Ashley Valle
Ziman, Benjamin
[et al.](#)

Publication Date

2021

DOI

10.3389/fmicb.2020.629526

Copyright Information

This work is made available under the terms of a Creative Commons Attribution License, available at <https://creativecommons.org/licenses/by/4.0/>

Peer reviewed



Epithelial Infection With *Candida albicans* Elicits a Multi-System Response in Planarians

Eli Isael Maciel^{1,2†}, Ashley Valle Arevalo^{1,2†}, Benjamin Ziman^{1,2}, Clarissa J. Nobile^{1,3*} and Néstor J. Oviedo^{1,3*}

¹ Department of Molecular & Cell Biology, University of California, Merced, Merced, CA, United States, ² Quantitative and Systems Biology Graduate Program, University of California, Merced, Merced, CA, United States, ³ Health Sciences Research Institute, University of California, Merced, Merced, CA, United States

OPEN ACCESS

Edited by:

Hector Mora Montes,
University of Guanajuato, Mexico

Reviewed by:

Delma S. Childers,
University of Aberdeen,
United Kingdom
Maria Rapala-Kozik,
Jagiellonian University, Poland

*Correspondence:

Néstor J. Oviedo
noviedo2@ucmerced.edu
Clarissa J. Nobile
cnobile@ucmerced.edu

† These authors have contributed
equally to this work

Specialty section:

This article was submitted to
Infectious Diseases,
a section of the journal
Frontiers in Microbiology

Received: 15 November 2020

Accepted: 22 December 2020

Published: 14 January 2021

Citation:

Maciel EI, Valle Arevalo A,
Ziman B, Nobile CJ and Oviedo NJ
(2021) Epithelial Infection With
Candida albicans Elicits
a Multi-System Response
in Planarians.
Front. Microbiol. 11:629526.
doi: 10.3389/fmicb.2020.629526

Candida albicans is one of the most common fungal pathogens of humans. Prior work introduced the planarian *Schmidtea mediterranea* as a new model system to study the host response to fungal infection at the organismal level. In the current study, we analyzed host–pathogen changes that occurred *in situ* during early infection with *C. albicans*. We found that the transcription factor Bcr1 and its downstream adhesin Als3 are required for *C. albicans* to adhere to and colonize the planarian epithelial surface, and that adherence of *C. albicans* triggers a multi-system host response that is mediated by the Dectin signaling pathway. This infection response is characterized by two peaks of stem cell divisions and transcriptional changes in differentiated tissues including the nervous and the excretory systems. This response bears some resemblance to a wound-like response to physical injury; however, it takes place without visible tissue damage and it engages a distinct set of progenitor cells. Overall, we identified two *C. albicans* proteins that mediate epithelial infection of planarians and a comprehensive host response facilitated by diverse tissues to effectively clear the infection.

Keywords: planarians, *Candida albicans*, infection, host–pathogen interactions, innate immune system, stem cells, animal models

INTRODUCTION

The innate immune system is the first line of defense against invading pathogens (Peiris et al., 2014; Espinosa and Rivera, 2016). The complex interactions between the pathogen and the host is a constantly evolving arms race, where the pathogen aims to invade and proliferate in the host, while the host aims to defend against infection. Both the host and pathogen responses to one another are known to be influenced by the physical presence of the infecting microorganism on specific host tissues, by the production of pathogen-associated virulence factors, and by the extent of host tissue damaged during the infection. Nonetheless, the underlying molecular mechanisms associated with these host–pathogen responses are largely unknown.

Candida albicans is an opportunistic human fungal pathogen that can cause both superficial mucosal and life-threatening systemic infections, particularly in immunocompromised individuals

(Filler, 2013; Pellon et al., 2020). *C. albicans* efficiently adapts to the dynamic host environment by quickly responding to host environmental cues, such as contact with epithelial cells, temperature, pH, nutrients, and iron levels (Brunke and Hube, 2014). *C. albicans* possesses a number of virulence traits that allow this pathogen to evade host innate immune defenses, such as the ability to change morphologies from the round budding yeast-form to the elongated hyphal form (Braun and Johnson, 1997; Mitchell, 1998; Saville et al., 2003). The yeast to hyphal transition is critical for *C. albicans* to invade and damage host tissues and to disseminate into the bloodstream (Wilson et al., 2016). Additionally, *C. albicans* can adhere to and colonize host tissues by forming recalcitrant biofilms on mucosal surfaces that provide physical protection from the host innate immune response (Nobile and Johnson, 2015; Valle Arevalo and Nobile, 2020).

Candida albicans uses two main strategies to invade and damage host epithelial cells. The first involves inducing endocytosis by host cells, while the second involves active physical penetration of host cells by *C. albicans* hyphal cells (Filler et al., 1995; Wachtler et al., 2012; Filler, 2013; Pellon et al., 2020). Adhering to epithelial cells and forming hyphae is the first step for *C. albicans* to invade host cells via either induced endocytosis or active physical penetration strategies (Wilson et al., 2016). For induced endocytosis, the process is mediated by fungal cell surface proteins (e.g., Ssa1 and Als3) that bind to cadherins on host cell surfaces (Nobile et al., 2006; Phan et al., 2007; Moreno-Ruiz et al., 2009; Sun et al., 2010; Filler, 2013). Active physical penetration of host cells by *C. albicans* cells, on the other hand, is a fungal-driven process that relies on the ability of hyphal cells to penetrate the epithelial cells without host activity (Wilson et al., 2016). Overall, the molecular mechanisms mediating both strategies are not fully understood.

To date, the analysis of host–pathogen interactions, including our understanding of pathogen invasion strategies, has been possible through the use of *in vitro*, *ex vivo*, and *in vivo* infection models. Work in *C. albicans* has led to the identification of several molecular players and signaling pathways involved in the host–pathogen response to acute *C. albicans* infections (Pellon et al., 2020). Nevertheless, the host response to infection likely goes beyond these localized interactions with the pathogen and may involve complex long-range intercellular communication between host tissues and organs to orchestrate an effective response against the invading pathogen (Godinho-Silva et al., 2019). Visualizing the complexity of the host response in real-time and integrating the contribution of different organs and systems has been challenging with currently available animal models (Chamilos et al., 2007; Mylonakis et al., 2007; Mylonakis, 2008; Pukkila-Worley et al., 2009; Glittenberg et al., 2011; Mallick et al., 2016; Bergeron et al., 2017; Gratacap et al., 2017; Peterson and Pukkila-Worley, 2018; Segal and Frenkel, 2018).

Previously, we introduced the planarian *Schmidtea mediterranea* as an *in vivo* infection model to study host–pathogen interactions with *C. albicans* (Maciel et al., 2019). We found that planarians can be conveniently infected by adding *C. albicans* cells directly into the media where planarians live, meaning that infection does not require invasive procedures, such as injections. This “passive” infection method allows for the

spatiotemporal tracing of *C. albicans* throughout the course of an infection, beginning with its initial interaction with the planarian epithelial surface. We showed that *C. albicans* forms hyphae after adhering to the planarian epithelial surface and that the aggressive invasiveness of *C. albicans* hyphal cells on planarian tissues is counteracted by the planarian innate immune response that eventually completely clears the infection in about a week (Maciel et al., 2019). Aside from prompting an innate immune response, infection of planarians with *C. albicans* triggers a mitotic response that is mediated by pluripotent adult stem cells known as neoblasts, the only somatic cell population in planarians with the capacity to divide (Maciel et al., 2019). This finding is intriguing because fungal infections have also been shown to activate mammalian stem cell proliferation, which is believed to potentiate the host innate immune response to infection (Yáñez et al., 2009, 2011; Megías et al., 2012, 2016; Yang et al., 2012). These findings suggest the possibility of evolutionary conservation of the host stem cell and innate immune responses between mammals and planarians. Nonetheless, the underlying mechanisms used by planarians to effectively clear *C. albicans* infections remain unclear.

In the present study, we show that infection of planarians with *C. albicans* triggers systemic waves of neoblast proliferation that can be detected within 6 h post-infection. These increases in neoblast proliferation are preceded by the adherence of *C. albicans* cells to the host epithelial cell surface. Furthermore, the presence of *C. albicans* elicits a reaction in planarians that resembles a regenerative response, including an increase in expression of the early growth response gene *Smed-egr2* (*egr2*), and an immediate wound response via the ERK signaling pathway (Wenemoser et al., 2012; Wurtzel et al., 2015; Owlarn et al., 2017). We also found that the host response is mediated by the *C. albicans* transcriptional regulator Bcr1 and its downstream cell surface protein Als3, which are key players in fungal cell adherence. Finally, we also observed that upon infection of planarians with *C. albicans*, there is an increase in expression of components of the Dectin signaling pathway within the host innate immune system, and an increase in the expression of host markers of neoblast subpopulations as well as markers of the nervous and excretory systems. Together, our findings demonstrate that the initial adherence of fungal cells to the epithelial surface of the planarian host elicits a multi-system response in the host involving the innate, excretory, and nervous systems, as well as neoblast function.

MATERIALS AND METHODS

Planarian Culture

The planarian colony used for all assays was CIW4, an asexual *S. mediterranea* strain. The colony was maintained as previously described (Oviedo et al., 2008b).

Microorganisms

The *C. albicans* wildtype strain SN250, a derivative of the clinical isolate SC5314, was used as the isogenic wildtype strain along

with the *bcr1* mutant strain (TF137) (Homann et al., 2009); the *als1* mutant strain and the *als3* mutant strain (Nobile et al., 2008); and the triple *sap1/sap2/sap3* mutant strain and the triple *sap4/sap5/sap6* mutant strain (Felk et al., 2002). All *C. albicans* strains were grown from cryogenic stocks on yeast extract peptone dextrose (YPD) agar for 48 h at 30°C. Single colonies were then inoculated into liquid YPD media and grown for 12–6 h at 30°C for use in the infection assays.

Infection Assays

Ten animals were kept in 6 mL wells with 4 mL of planarian water (media) containing 25 million *C. albicans* cells per milliliter as previously described (Maciel et al., 2019). The animals were kept in the infected media until collected for specific experiments at various timepoints. The infection assay took place at 25°C, the preferred temperature for planarians, for the duration of the experiments.

C. albicans CFU Measurements

Planarians were collected at the indicated timepoints during the infection and rinsed with planarian media. The animals were homogenized in 500 µL of planarian media and diluted in 10 mL of planarian media. After homogenization, 300 µL of the homogenate was plated onto YPD media agar plates containing a cocktail of broad-spectrum antibiotics. The colonies were counted to obtain CFUs after being incubated at 30°C for 48 h.

Protein Extractions

Animals were washed thoroughly prior to being placed in 1.5 mL centrifuge tubes. Approximately 150 µL of 1X RIPA Buffer (Cell Signaling Technologies, 9806) containing protease inhibitors [Complete Mini Protease Inhibitor Cocktail (Roche, 04693124001); Halt Phosphatase Inhibitor cocktail (Thermo Scientific, 1862495), 1 mM PMSE, 1 mM DTT] was added to each tube. Samples were placed on ice and homogenized using a motorized pestle (Fisher, 12-141-361) for 10 s, followed by a 45-min incubation. Samples were then centrifuged at 20,817 g for 20 min at 4°C. Approximately 100 µL of supernatant was transferred into a clean tube and placed on ice. Protein concentrations were determined using a Bradford protein assay (VWR, E530-1L). In a 1.5 mL tube, 50 µg of supernatant was mixed with 6× Laemmli buffer (6% SDS, 9% β-mercaptoethanol, 4.8% glycerol, 0.03% bromophenol blue, 375 mM Tris-HCl) and was heated to 94°C for 10 min to denature and reduce the proteins.

Western Blots

Protein lysate mixtures were loaded onto a 15% SDS-PAGE gel along with a molecular weight marker (Thermo Scientific, 26619). Samples were transferred to a methanol-activated PVDF membrane (Bio-Rad, 162-0175) for 2 h at 55 V in a 1× Tris-glycine transfer buffer [25 mM Tris base, 192 mM glycine, 10% (v/v) methanol] on ice. The membrane was blocked with 5% BSA in TBST (20 mM Tris-base, pH 7.6, 140 mM NaCl, 0.1% Tween-20) for 2 h at room temperature and incubated with the primary antibody dilutions for 16 h at 4°C on a

rocker. The primary antibodies used were anti-actin (1:3000; Developmental Studies Hybridoma Bank, JLA20), anti-pERK (1:400; a gift from the Bartscherer lab) (Owlarn et al., 2017). The primary antibody was removed and the membrane was washed with TBST four times (5 min each wash), before the addition of the secondary antibody: goat-anti-rabbit HRP IgG antibody (1:10,000; Abcam, ab7097) for anti-ERK, goat-anti-mouse HRP IgG antibody (1:10,000; Invitrogen, G-21040) for anti-actin. Secondary antibody dilutions were incubated for 1 h at room temperature with 5% non-fat milk in TBST-SDS (20 mM Tris-base, pH 7.6, 140 mM NaCl, 0.2% Tween-20, 0.01% SDS). The membrane was washed with TBST four times (5 min each wash), followed by two 5-min washes with 1X PBS. The addition of the HRP chemiluminescence substrate (Millipore, WBLUF0100A) allowed for the detection of a signal. For the removal of primary antibody pERK, blots were stripped for 15 min (Thermo Scientific, 21059) and washed with 1× PBS four times (5 min each wash) before blocking for actin. Band intensities were quantified by computing the area under the curve using imageJ software bundled with Java (Schneider et al., 2012). pERK activity was then normalized to actin. Blots were imaged using a ChemiDoc gel imaging system (Bio-Rad).

Whole-Mount Immunofluorescence

Non-infected and infected planarians were sacrificed with 5.7% 12N HCL solution for 5 min and fixed using Carnoy's solution for 2 h on ice. After the fixation, animals were stored in methanol at –20°C and then bleached overnight in a 6% H₂O₂ solution. Animals were then rehydrated in dilutions of methanol:PBSTx and stained as previously described (Ziman et al., 2020). The primary antibody used was α-H3p, 1:250 (Millipore Cat# 05–817R). The secondary antibodies used were goat anti-rabbit Alexa568, 1:800 (Invitrogen Cat# 11036) and HRP-conjugated goat anti-rabbit antibody (Millipore Cat# 12-348).

To stain *C. albicans* cells, infected animals were sacrificed in 10% NAC diluted in PBS. The planarians were then fixed in 4% formaldehyde in PBTx and permeabilized in 1% SDS. The animals were bleached in 3% H₂O₂ in 1× PBS. The primary antibody used was anti-*Candida*, 1:500 (Thermo Fisher Cat# PA1-27158). The secondary antibody used was goat anti-rabbit Alexa568, 1:800 (Invitrogen Cat# 11036).

RNAi Treatments

Double-stranded RNA (dsRNA) was synthesized as previously described (Oviedo et al., 2008a). The dsRNA was applied via microinjections in three consecutive days with a fourth injection a week after the last injection. The animals were starved for at least 1 week prior to the dsRNA injections.

Whole-Mount Fluorescence *in situ* Hybridizations

Riboprobes were made using T3 and T7 polymerases and a digoxigenin-labeled ribonucleotide mix (Roche, Cat. # 11277073910) using PCR templates, as described previously (Pearson et al., 2009). *In situ* hybridization with and

without fluorescence was performed as described previously (King and Newmark, 2013).

Imaging and Data Processing

Area measurements and cell counts were calculated using imageJ software bundled with Java (Schneider et al., 2012). The Nikon AZ100 Multizoom microscope was used to collect the digital images and the images were processed using NIS Elements AR3.2 software (Nikon). Photoshop software (Adobe) was used to adjust contrast and brightness.

Gene Expression Analyses

RNA was extracted using TRIzol (Thermo Fisher Scientific). qRT-PCR reactions were performed using SYBR Green Master Mix in a 7500 Fast Real Time PCR cycler (Applied Biosystems). The TATA-box-binding protein domain gene was used as the internal control. Each experiment was performed in triplicate for each timepoint. qRT-PCR was performed as previously described (Peiris et al., 2012).

Cell-Free Filter Sterilized Planarian Media

The media from 6 hpi infection assays was removed from the planarian wells and filter sterilized using a Corning vacuum system with 0.22 μm pore-size 13.6 cm^2 PES Membrane (Cat. # 431153). Uninfected animals were then inoculated with the cell-free filter sterilized media using the infection assay described above.

Statistical Analyses

Two-way ANOVA or *t*-test statistics were performed as indicated in the figure legends, and data are shown as the mean \pm SEM or fold change \pm SEM unless otherwise noted. Logrank statistical tests were performed for the survival curves as indicated in the figure legends. All statistics were performed by pooling biological replicates from each technical replicate using Prism7, Graphpad software Inc.¹.

RESULTS

Adherence of *C. albicans* to the Planarian Epithelial Surface Initiates an Early Wound-Like Response

To assess the host response to *C. albicans* infection, planarians were infected with a lethal concentration (25×10^6 cells/mL) of *C. albicans* cells via soaking as previously described (Maciel et al., 2019). Our prior results demonstrated that planarians responded to fungal infection with an increase in mitotic activity; however, it was unclear when during the infection this fungal-induced proliferative response was occurring (Maciel et al., 2019). To address this, we infected planarians with *C. albicans* and analyzed host mitotic activity temporally over the course of 48 h (Figures 1A,B; see Supplementary Figure 1 for descriptions

of the spatial orientations of the planarian whole mounts). We observed no host behavioral or macroscopic differences within the first 48 h post-infection (hpi) between the uninfected and experimental groups. We did, however, detect two host mitotic peaks occurring at six and 24 hpi, which were preceded by decreased mitotic activity (Figure 1B). The largest burst in mitotic activity ($\sim 150\%$) was observed 6 hpi, and was spatially increased throughout the planarian body, suggesting a system-wide neoblast response (Figures 1A,B).

To determine if the mitotic response was due to the adherence or penetration of *C. albicans* cells through the epithelial surface of planarians, we focused on early timepoints of 1, 3, and 6 hpi. These experiments revealed that as early as 1 hpi, *C. albicans* cells began to adhere to the planarian epithelial surface and that by 6 hpi, the fungal cells were readily clustered throughout the epithelial surface (Figure 1C). The increased presence of *C. albicans* cells on the planarians during these early timepoints was determined by macerating planarians and measuring colony forming units (CFUs) after plating the homogenized slurry on agar plates. We found that in the first 6 hpi, the number of *C. albicans* cells increased by two orders of magnitude (i.e., ~ 10 CFUs at 1 hpi compared to $\sim 1,000$ CFUs at 6 hpi) (Figure 1D). To discern if the increase in *C. albicans* cells during this early infection was limited to the superficial adherence of *C. albicans* cells to the host epithelial surface or to penetration of *C. albicans* cells into host tissues, we performed immunostaining on transverse cross sections using an antibody specific for *C. albicans*. We found that *C. albicans* cells were adhered to the epithelial surface of the planarians, while no *C. albicans* antibody signal was detected in deep tissues even after 6 hpi (Figure 1E and Supplementary Figure 2). This finding is consistent with previous results demonstrating that *C. albicans* cells attach to the host epithelial surface during early timepoints of infection (Maciel et al., 2019).

In response to physical injury, planarians have been shown to elicit a regenerative mitotic response occurring 6 h post-injury (Saló and Bagueña, 1984; Wenemoser and Reddien, 2010). Due to the apparent overlap between injury stimuli (i.e., the presence of penetrating *C. albicans* hyphal cells) and the mitotic response observed during the early infection period (6 hpi), we hypothesized that invading *C. albicans* hyphal cells could trigger a wound response in planarians during early infection.

In response to injury in planarians, the planarian extracellular regulated kinase (ERK) becomes activated via phosphorylation (pERK), and is among the earliest events essential for regeneration initiation, occurring ~ 15 min post-injury (Owlarn et al., 2017). We, therefore, measured pERK protein levels at early infection timepoints using a western blot and found that there was a gradual increase in pERK levels, as early as 30 min post-infection (\sim threefold increase), which increased to about fourfold by 6 hpi (Figure 1F). We also measured the post-infection expression levels of *Smed-runt1* (*runt1*) and *Smed-egr2* (*egr2*), two early wound response genes in planarians (Sandmann et al., 2011; Wenemoser et al., 2012; Wurtzel et al., 2015; Owlarn et al., 2017). We observed an increase in the expression of *egr2* (\sim twofold) over the first 48 hpi (Figure 1G). Intriguingly, *runt1* was either slightly reduced or showed no changes in expression

¹<http://www.graphpad.com>

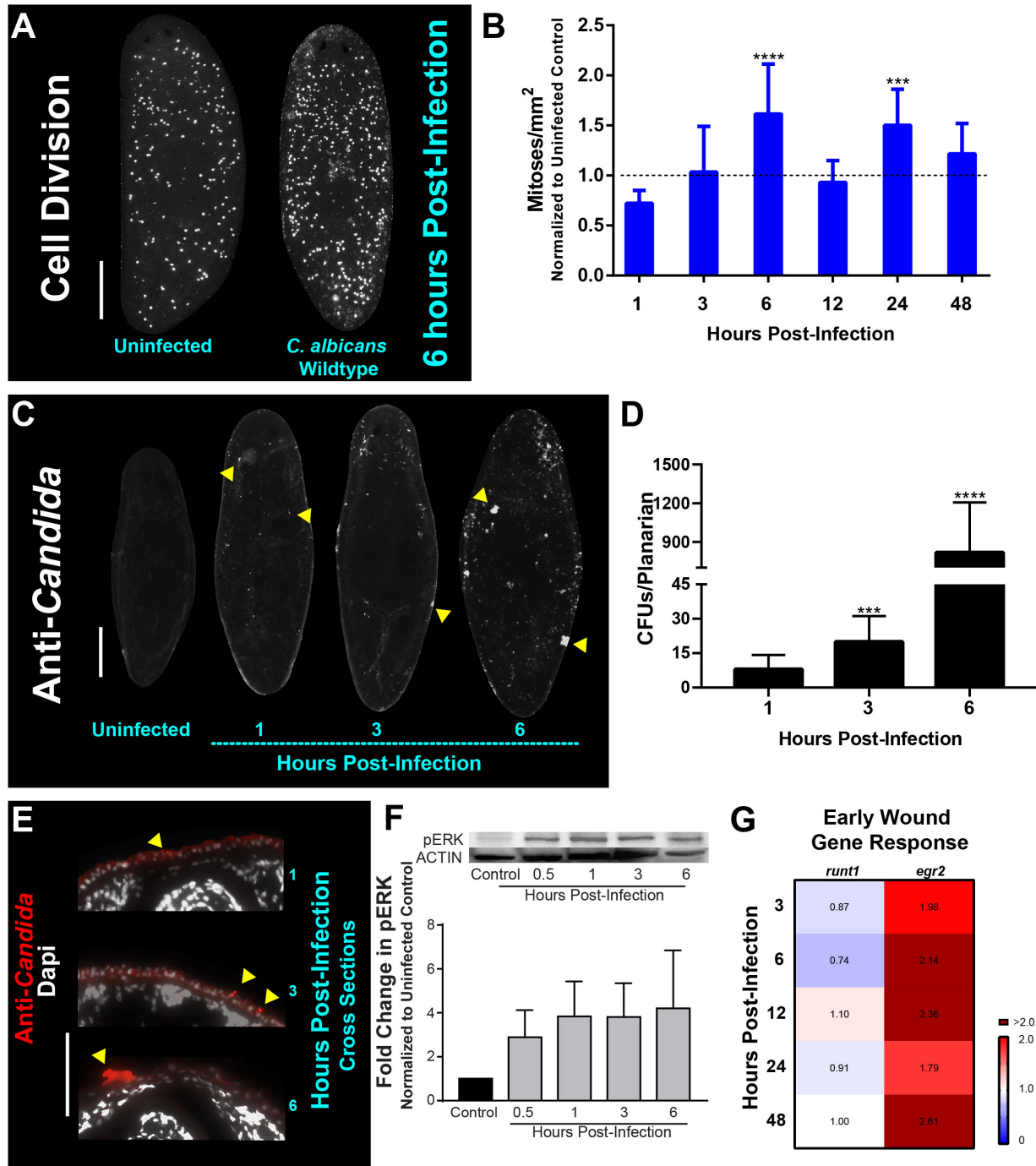


FIGURE 1 | *Candida albicans* infection leads to an early wound and mitotic response in planarians. **(A)** Whole-mount immunostaining with anti-phospho-histone H3 (ser10) antibody for planarians, which labels mitotic cells (white foci) at 6 h post-infection with the *C. albicans* wildtype strain. **(B)** Number of mitoses in response to *C. albicans* cells between one to 48 h normalized to an uninfected planarian. **(C)** Whole-mount anti-*Candida* antibody stain at 1, 3, and 6 h post-infection (white foci). Yellow triangles indicate notable *C. albicans* aggregates. **(D)** *C. albicans* colony forming units (CFUs) normalized per planarian. Ten animals per infection timepoint were used. **(E)** Transverse cross section images from the dorsal side of the planarian body showing the adherence of the *C. albicans* wildtype strain (red signal) at 1, 3, and 6 h post-infection. Yellow triangles indicate notable *C. albicans* aggregates. **(F)** Western blot of planarian phosphorylated-ERK (p-ERK) and quantification at different timepoints of a *C. albicans* infection. β -tubulin was used as an internal control. **(G)** Gene expression levels represented in a heat map of wound-induced response planarian genes *run1* and *egr2* at the different infection timepoints. Gene expression is represented by fold change normalized to an uninfected control. Color scale depicts red as upregulation and blue as downregulation; burgundy demonstrates upregulation greater than twofold. Data were obtained in triplicate per experiment for at least two biological and technical replicates. *C. albicans* infections were performed using 25 million cells/mL. All graphs represent mean \pm SEM. Statistical comparisons are against the uninfected control. Scale bar is 200 μ m. Two-way ANOVA, *** $P < 0.001$, **** $P < 0.0001$.

over the first 48 hpi (Figure 1G). Overall, these results suggest that the adherence of *C. albicans* cells to the epithelial surfaces of planarians shortly after infection triggers a regenerative wound-like response in the host.

Als3 and Bcr1 Are Required for *C. albicans* to Adhere to and Colonize the Planarian Epithelial Surface

Next, we sought to test if the dynamics of infection in planarians can be modulated by genetically disrupting *C. albicans* virulence factors known to contribute to disease progression in the host (Mayer et al., 2013). Based on our observations that *C. albicans* adheres to planarians in order to invade them, we decided to focus our attention on *C. albicans* virulence factors associated with adherence and biofilm formation. The agglutinin-like sequence (Als) family of cell surface glycoproteins are important *C. albicans* adhesins that mediate cell–cell and cell–substrate adherence (Hoyer and Cota, 2016). Two major Als proteins that are known to be important for adherence and biofilm formation are Als1 and Als3 (Nobile et al., 2006, 2008). In addition to these two adhesins, a known master regulator of *C. albicans* biofilm formation that controls the expression of *ALS1* and *ALS3* is Bcr1 (Nobile and Mitchell, 2005; Nobile et al., 2006, 2012). We, therefore, assessed the ability of the *als1*, *als3*, and *bcr1* mutant strains to infect planarians. In addition to adherence, *C. albicans* also produces secreted aspartyl proteases (Saps) that are important virulence factors in causing host cell damage (Naglik et al., 2003; Mayer et al., 2013). We, therefore, also assessed the ability of two triple deletion SAP mutant strains (encompassing the major SAPs involved in virulence), the *sap1/sap2/sap3* and the *sap4/sap5/sap6* mutant strains, to infect planarians.

To our surprise, we found that all *C. albicans* mutant and wildtype strains were capable of adhering to the planarian epithelial surface. Qualitatively, it appeared that the *als3* and *bcr1* mutant strains displayed less adherence 6 hpi (Figure 2A). Consistent with this observation, our results revealed an increase in the survival of planarians when they were infected with lethal doses of the *als3* and *bcr1* mutant strains compared to the wildtype strain (Figure 2B). Additionally, we discovered that when the *C. albicans* wildtype strain came into contact with planarians, there was a dramatic increase in the gene expression levels of *ALS1*, *ALS3*, and *BCR1* (Figure 2C). Overall, these results suggest that fungal cell adherence mediated by the adhesin Als3 and the transcription factor Bcr1 is important for *C. albicans* to colonize the epithelial surface of planarians during an infection.

Als3 and Bcr1 Are Important Players in the Planarian Mitotic Response to *C. albicans* Infection

Given the importance of *C. albicans* Als3 and Bcr1 for colonization of the planarian epithelial surface, we next wanted to know whether Als3 and Bcr1 play roles in the mitotic response of planarians. We found that 6 hpi, all *C. albicans* mutant and wildtype strains were capable of mounting a mitotic response in planarians; however, infection with the *als3* and *bcr1*

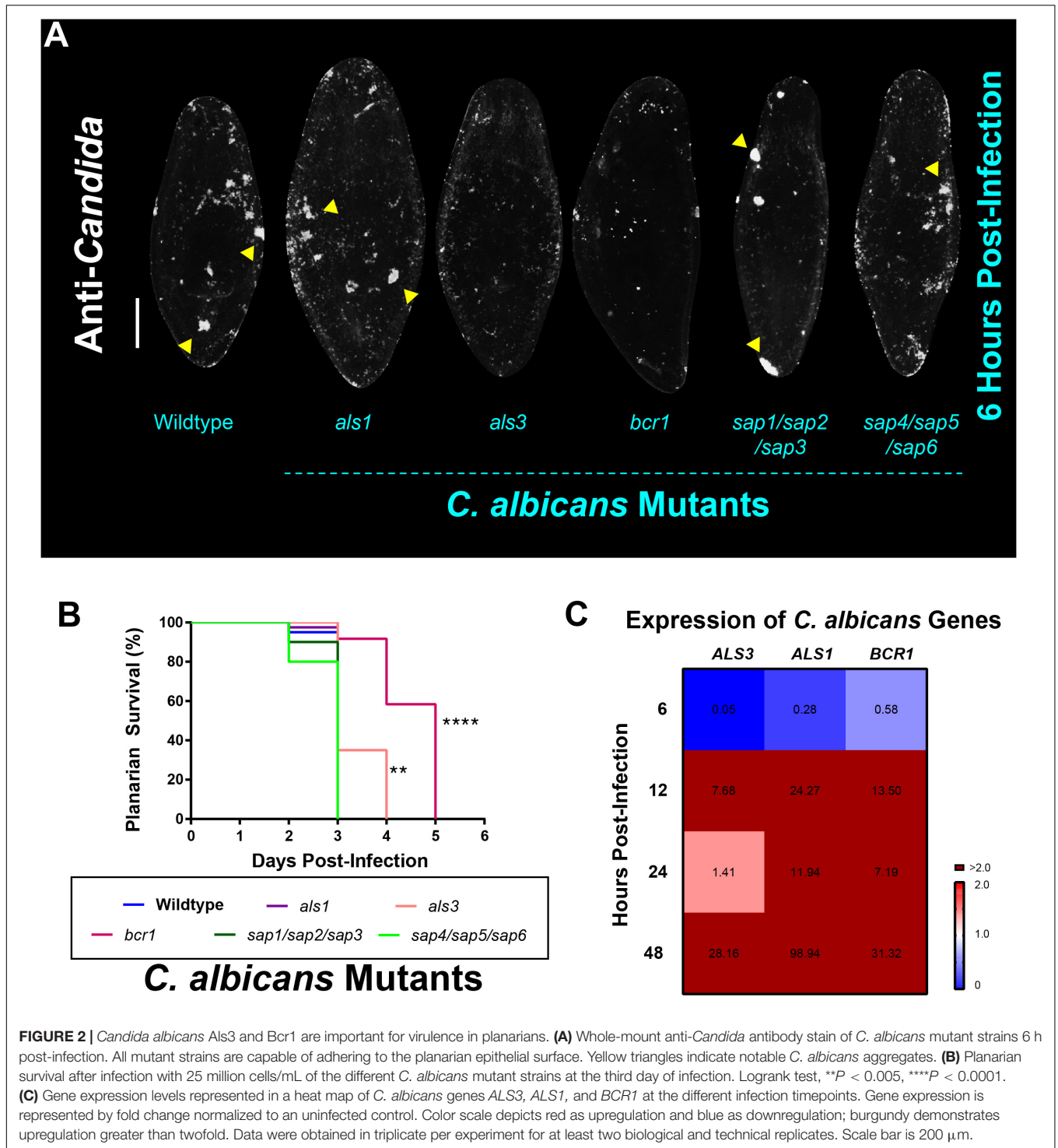
mutant strains displayed significantly less mitotic proliferation in planarians than that of the wildtype strain (Figures 3A,B). These findings indicate that Als3 and Bcr1 are involved in mediating the planarian mitotic response.

Since secreted aspartyl proteases (Saps) are important *C. albicans* virulence factors, we hypothesized that Saps may play roles in the planarian host response to *C. albicans* infection. To address this, we exposed planarians to cell-free filter sterilized media obtained from 6 hpi infection assays and measured planarian mitotic activity. We found no difference in the mitotic activity between uninfected animals and the group exposed to filter sterilized media from the infection assays, suggesting that the increase in cell proliferation upon *C. albicans* infection requires the physical presence of the pathogen (Figures 3C,D). Altogether, these findings suggest that adherence of *C. albicans* cells to the planarian epithelial surface, rather than fungal secreted proteases, induces the host mitotic response during the early hours post-infection.

The Planarian Dectin Signaling Pathway Modulates the Early Mitotic Response to and the Clearance of the Fungal Infection

In order to understand how *C. albicans* cells interact with the planarian host to trigger hyper-proliferation, we decided to explore the initial molecular response mediated by the planarian innate immune system upon infection. Our previous work showed that the expression of genes in the host Dectin signaling pathway are generally upregulated 1 day post-infection with *C. albicans* (Maciel et al., 2019). To expand on these initial findings, we screened, by qRT-PCR, an expanded list of host genes encoding components of the Dectin signaling pathway, including the gene encoding the upstream SYK adapter protein *Smed-syk* (*syk*) and downstream gene components *Smed-card* (*card*), *Smed-bcl* (*bcl*), *Smed-malt1* (*malt1*), *Smed-tab1* (*tab1*), and *Smed-tak* (*tak*) during early infection with *C. albicans* (Wagener et al., 2018). We found that as early as 3 hpi there was a significant increase in the expression of all genes assayed of the Dectin signaling pathway, and that the upregulation of each gene was generally sustained for 48 hpi (Figure 4A). Notably, the upstream gene *syk* displayed an increase in expression (~threefold) in the first 6–12 hpi. We confirmed this upregulation in expression using fluorescent *in situ* hybridization (FISH) with a probe against *syk*, which revealed *syk* expression throughout the animal with enrichment in the digestive system including the pharynx of uninfected planarians (Figure 4B). In the infected planarians, we observed that *syk* expression became more prominent with the appearance of punctate foci readily visible in the main intestinal branches close to the brain at 6 hpi (observed in 6 out of 8 animals).

To assess the role of the Dectin signaling pathway in the planarian innate immune response, we disrupted *syk* function with RNA-interference (RNAi) and evaluated the planarian mitotic response and ability to clear the *C. albicans* infection. Intriguingly, downregulation of *syk* by RNAi led to a slight increase (13%) in mitotic activity when compared to the infected



control at 6 hpi (Figures 4C,D). Loss of *syk* function by RNAi resulted in planarians having a reduced capacity to clear the infection, even after 12 days post-infection (Figures 4E,F). Taken together, these findings suggest that the Dectin signaling pathway is an important mediator of the innate immune response in planarians that modulates the early mitotic response to fungal infection and is required for proper clearance of the infection.

C. albicans Infection Triggers a Heterogenous Transcriptional Response Across Planarian Neoblast Subpopulations

Recent work suggested a model in which transcriptomic changes occur in planarian neoblasts as they adopt new cellular identities

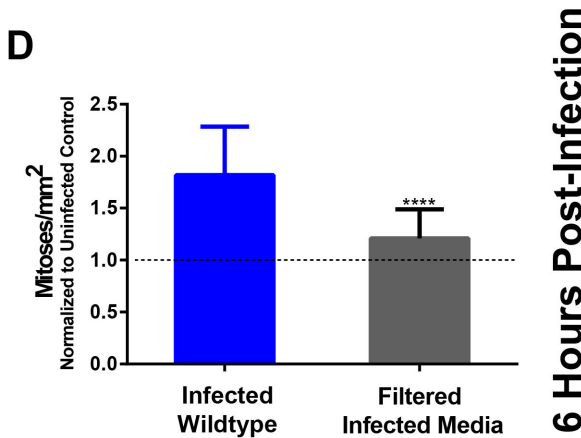
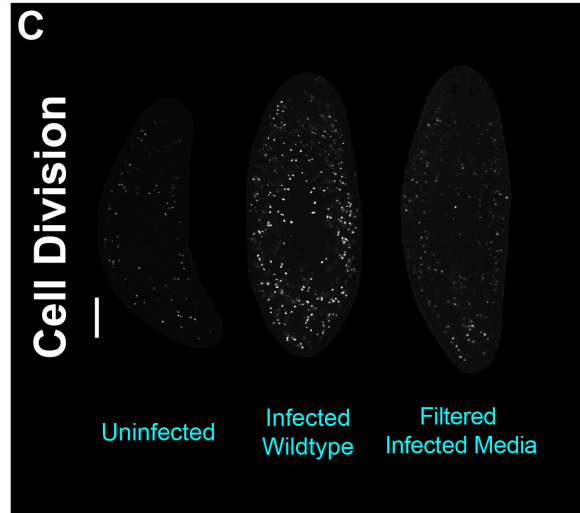
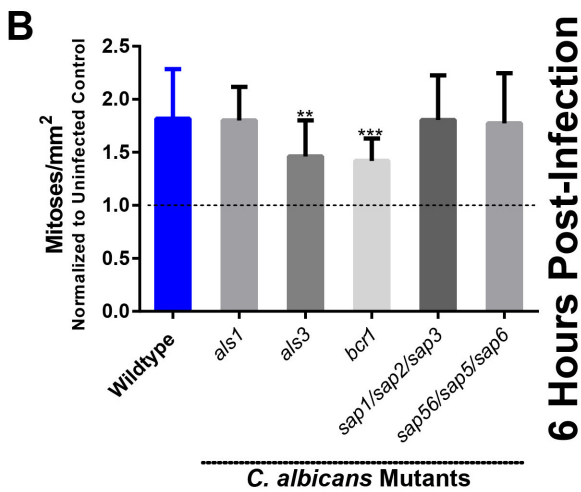
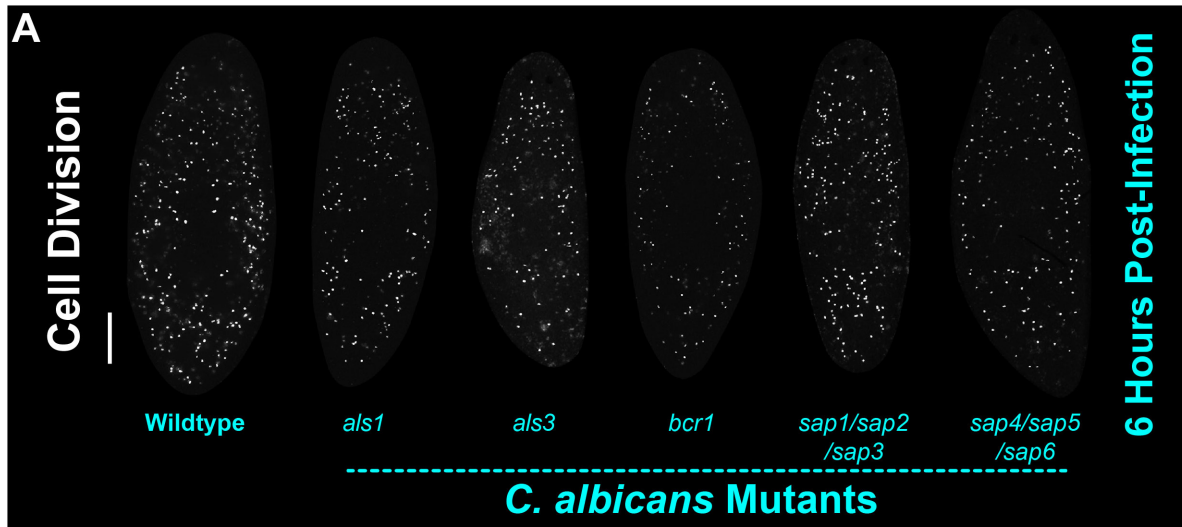


FIGURE 3 | The planarian mitotic response decreases in infections with less virulent *C. albicans* *als3* and *bcr1* mutant strains. **(A)** Whole-mount immunostaining with anti-phospho-histone H3 (ser10) antibody for planarians, which labels mitotic cells (white foci) at 6 h post-infection with the *C. albicans* mutant strains indicated. **(B)** Number of mitotic cells in response to *C. albicans* mutant strains normalized to uninfected planarians at 6 h post-infection. **(C)** Whole-mount immunostaining with anti-phospho-histone H3 (ser10) antibody for planarians, which labels mitotic cells (white foci) at 6 h post-infection for animals that were soaked in filter sterilized cell-free infected planarian media. **(D)** Whole mount immunostaining with anti-phospho-histone H3 (ser10) antibody, which labels mitotic cells (white foci) at 6 h post-infection normalized to an uninfected control. *C. albicans* infections were performed using 25 million cells/mL. Graphs represent mean \pm SEM. All statistical comparisons are against the wildtype strain unless noted with bars. Scale bar is 200 μ m. Two-way ANOVA, ** $P < 0.005$, *** $P < 0.001$, **** $P < 0.0001$.

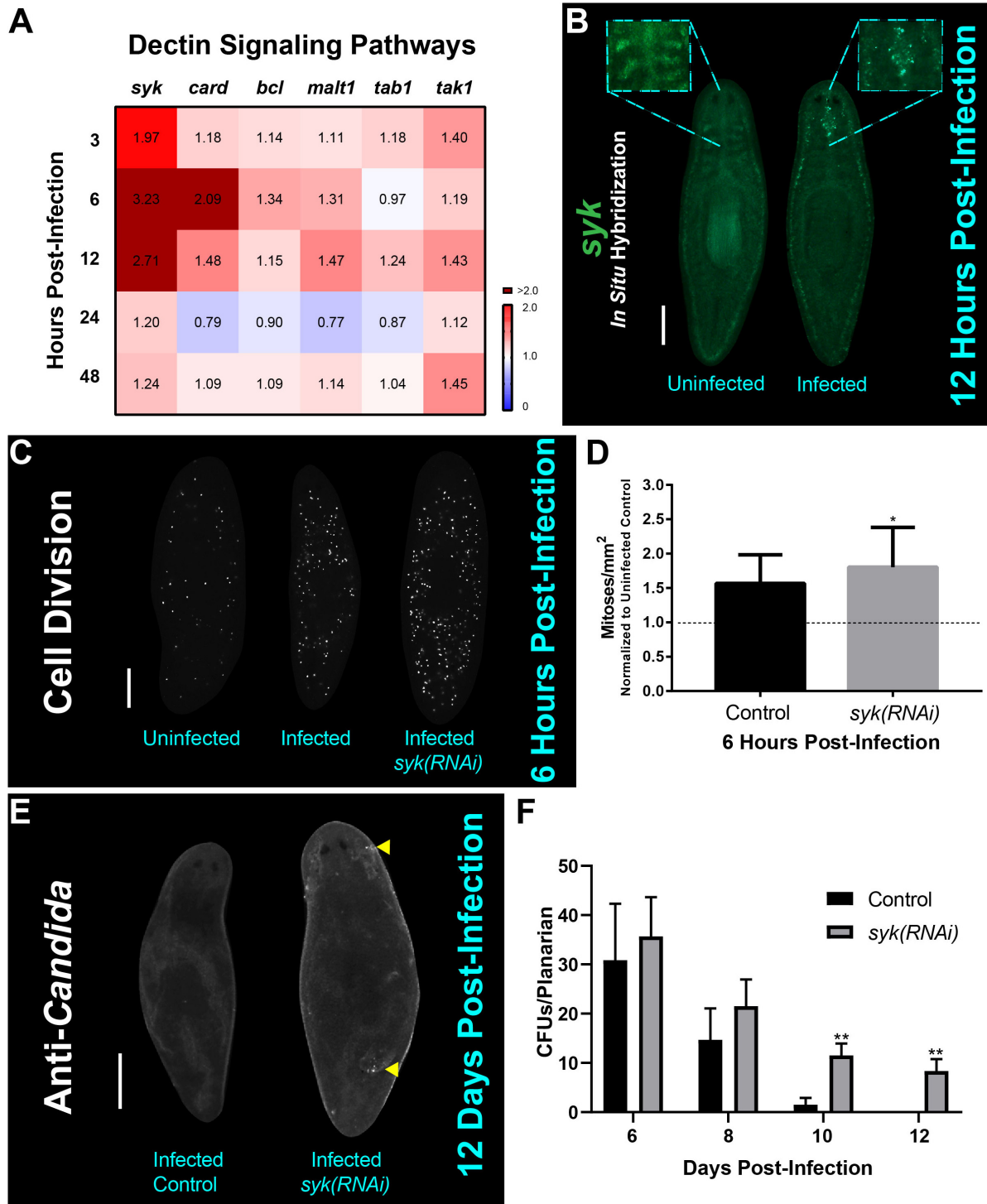


FIGURE 4 | The Dectin signaling pathway plays a role in the host response to and clearance of *C. albicans* infection. **(A)** Gene expression levels for Dectin signaling pathway homologs at early and late timepoints of *C. albicans* infection using 25 million *C. albicans* cells/mL. Gene expression is represented in a heat map displaying fold change normalized to an uninfected control. Color scale depicts red for upregulation and blue for downregulation; burgundy demonstrates upregulation over twofold. Data were obtained in triplicate per experiment for at least two biological and technical replicates. **(B)** Fluorescent *in situ* hybridization showing expression of *syk* in an uninfected and 12-h infected animal. The boxed regions are magnifications of representative uninfected and infected animals. This experiment was replicated two times using five animals per experiment. Scale bar is 200 μ m. Images are representative of eight animals for at least two biological and technical replicates. **(C)** Whole mount immunostaining with anti-phospho-histone H3 (ser10) antibody, which labels mitotic cells (white foci) at 6 h post-infection. **(D)** Number of mitoses of control infected animal versus *syk(RNAi)* infected animals normalized to an uninfected control at 6 h post-infection. **(E)** Representative images of whole (Continued)

FIGURE 4 | Continued

mount anti-*Candida* antibody stain at 12 days post-infection (white foci) of a control animal and *syk(RNAi)* animal. Yellow triangles indicate notable *C. albicans* aggregates. **(F)** Number of *C. albicans* colony forming units (CFUs) normalized per planarian of infected control versus infected *syk(RNAi)* planarians throughout the course of infection. This experiment was replicated two times using five animals per experiment. 25 million *C. albicans* cells/mL was used for the infections. All graphs represent mean \pm SEM. Scale bar is 200 μ m. T-test, * $P < 0.01$, ** $P < 0.005$.

necessary to support cellular turnover and tissue regeneration (Zeng et al., 2018). To gain a deeper understanding of how neoblast dynamics are affected in response to *C. albicans* infection, we screened, by qRT-PCR, planarian genes encoding neoblast markers for various subpopulations of progenitor cells. We measured changes in gene expression for six different neoblast lineages at different timepoints post-infection, and our results revealed that transcriptomic changes were not homogenous throughout the neoblast subpopulations. We discovered an upregulation in the expression of several neoblast subclasses detected as early as 3 hpi and this upregulation was maintained for the next 48 hpi (Figure 5A). The neoblast lineages measured represent 12 neoblast clusters of cells (NB1–NB12) and are ordered based on *Smed-piwi-1* (*piwi-1*) transcript levels; thus, NB1 expresses higher levels of *piwi-1* relative to NB12 (Zeng et al., 2018). We found that in the first 24 hpi there was a reduction in the expression of *Smed-tspan-1* (*tspan-1*), which defines the NB2 subpopulation that contains the pluripotent clonogenic neoblasts (cNeoblasts) (Figure 5A) (Wagner et al., 2011; Zeng et al., 2018). The expression of *tspan-1* was slightly increased at 48 hpi. We also found that expression of the *Smed-lmo3* (*lmo3*) marker (NB3) was consistently downregulated throughout the first 48 hpi. Overall, we detected the highest expression levels associated with markers of the neoblast subpopulations NB9, NB11, NB4, NB7, and NB5. The absolute highest expression levels were detected with the marker *Smed-pou2-3* (*pou2-3*) (NB9), which gradually increased after 3 hpi and peaked more than eightfold at 48 hpi (Figure 5A). High expression levels were also detected for markers *Smed-ston2* (*ston2*) and *Smed-pdch11* (*pdch11*) (NB11 and NB4, respectively). Of note, *Smed-pj-1b* (*pj-1b*) of the NB4 neoblast subpopulation was the only marker whose expression increased dramatically while the other eight NB4 markers remained close to the levels of the control (Figure 5B). Altogether, these results suggest that infection with *C. albicans* triggers a heterogenous transcriptional response across planarian neoblast subpopulations.

C. albicans Infection Modulates Transcription Within Neuronal Clusters and the Excretory System of Planarians

To further examine how increased gene expression levels of the NB9 and NB11 neoblast subpopulations impact the planarian response to infection with *C. albicans*, we extended our analysis to include markers of downstream planarian progenitor cells that lead to differentiated cells in the excretory and nervous systems (Rink et al., 2011; Ross et al., 2017; Zeng et al., 2018). The early progenitors of the nervous (NB11) and excretory (NB9) systems were upregulated during infection with *C. albicans* (Figure 5A), suggesting that the planarian infection response

goes beyond neoblast subpopulations to also involve post-mitotic committed cells.

The planarian central nervous system is comprised of distinct neural subtypes, labeled by the synthesis of neurotransmitters that they produce (Ross et al., 2017). These subtypes include dopaminergic, octopaminergic, GABAergic, serotonergic, and cholinergic neurons, which all have specific markers [*Smed-th* (*th*), *Smed-tbh* (*tbh*), *Smed-gad* (*gad*), *Smed-tph* (*tph*), and *Smed-chat* (*chat*), respectively]. We wanted to understand how the increase in expression of NB11 upon *C. albicans* infection would impact the different neuronal subpopulations. To explore this idea, we measured the expression levels, by qRT-PCR, of these six neural markers at both 12 and 24 hpi, which were the timepoints where the expression of NB9 and NB11 were highest (Figure 5A). We found that the expression levels for two neuron subtypes, *tbh* and *chat* were increased when compared to uninfected animals, with *chat* displaying the highest levels of upregulation (Figure 6A). We confirmed our qRT-PCR results by performing FISH using a *chat* probe, which is expressed along the brain and the ventral cords in uninfected planarians. The *chat* signal was found to be increased in the brain of infected planarians starting at 3 hpi (Figure 6B). We also found that the increase in expression of *chat* and the downstream adapter gene *syk* of the Dectin signaling pathway can be detected as early as 15–30 min post-infection and remains elevated for the first 3 hpi (Figure 6C). The expression levels of both *chat* and *syk* were observed to increase at 30 min and continued to increase in the later timepoints of infection.

To determine how the planarian excretory system is impacted by the increase in NB9 expression, we measured markers of the protonephridia, and more specifically, markers of the flame cells that contribute to electrolyte balance and mucus production, among other excretory functions (Rink et al., 2011). We observed an increase in expression of the markers of collecting ducts *Smed-slc9a-3* (*slc9a-3*), distal tubules *Smed-slc4a-6* (*slc4a-6*), and proximal tubules *Smed-slc6a-13* (*slc6a-13*) during the first 24 hpi (Figure 6D). We validated these results by performing FISH using a *Smed-inx10* (*inx10*) probe (Oviedo and Levin, 2007), which confirmed a steady increase in *inx10* expression throughout the planarian body at 24 hpi (Figure 6E). Overall, these findings suggest that both the nervous and excretory systems contribute to the host response during fungal infection.

DISCUSSION

Here, we show that the planarian infection model is an advantageous animal model system to study host–pathogen interactions, particularly at early stages of epithelial infection

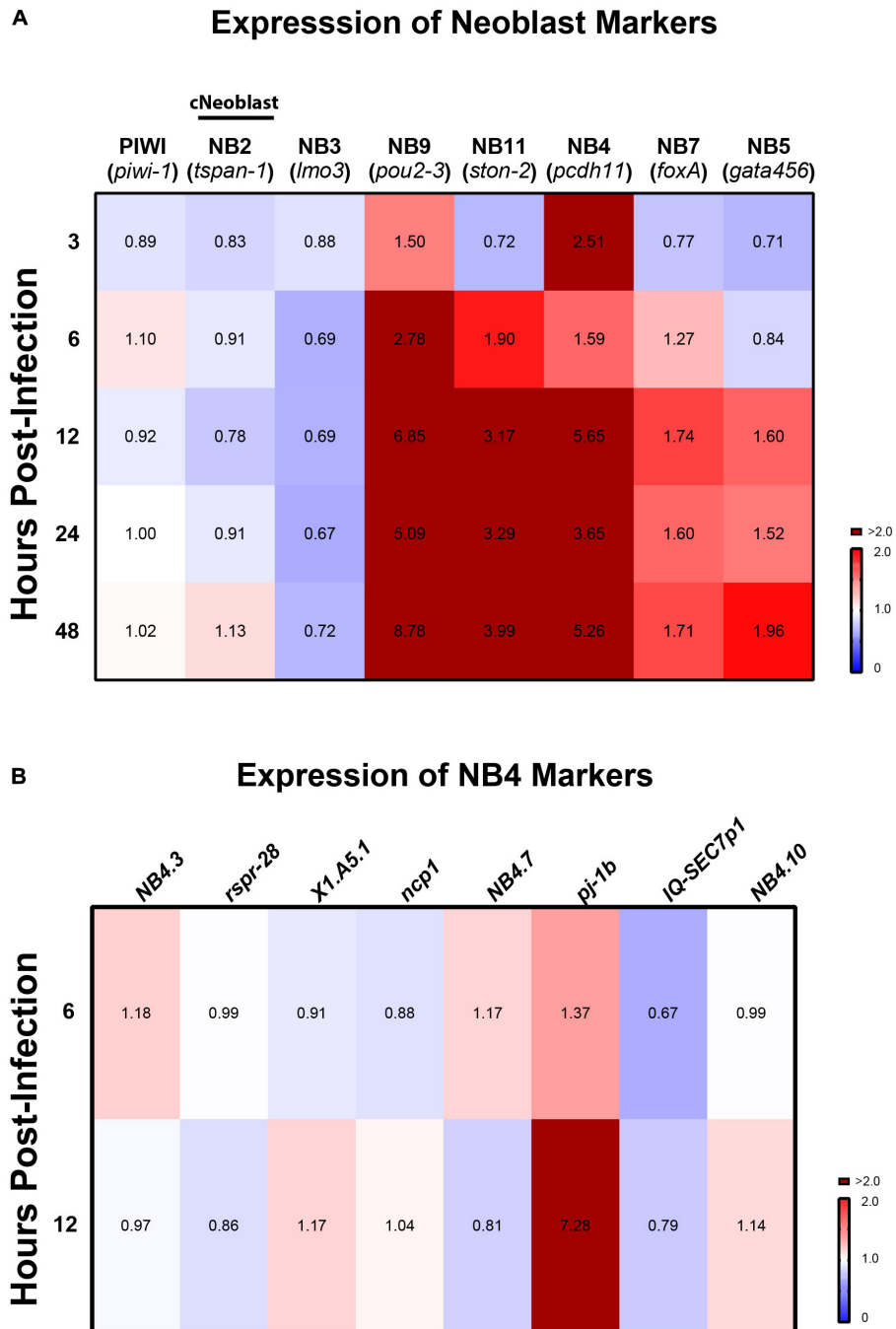


FIGURE 5 | Expression of planarian neoblast subclasses throughout infection with *C. albicans*. **(A)** Gene expression levels of neoblast markers and subclass markers of clonal neoblasts over the course of *C. albicans* infection. Expression levels are represented in a heat map, where the color scale depicts red as upregulation and blue as downregulation; burgundy is upregulation greater than twofold. Gene expression is represented by fold change normalized to an uninfected control. Gene expression values represent triplicate samples for at least two biological and technical replicates. **(B)** Gene expression of eight other markers for NB4 (Zeng et al., 2018).

with *C. albicans*. Our results demonstrate that the superficial adherence of *C. albicans* to the planarian epithelial surface triggers a multi-system host response involving stem cells and differentiated tissues in the planarian (Figure 7). These findings underscore the advantages of analyzing host–pathogen

interactions *in situ* as a powerful paradigm to identify crosstalk between tissues during fungal infection. Planarians are thus a unique model system to study the host response to infection at the organismal level, a feature that is largely missing from or challenging to achieve with existing animal models of infection.

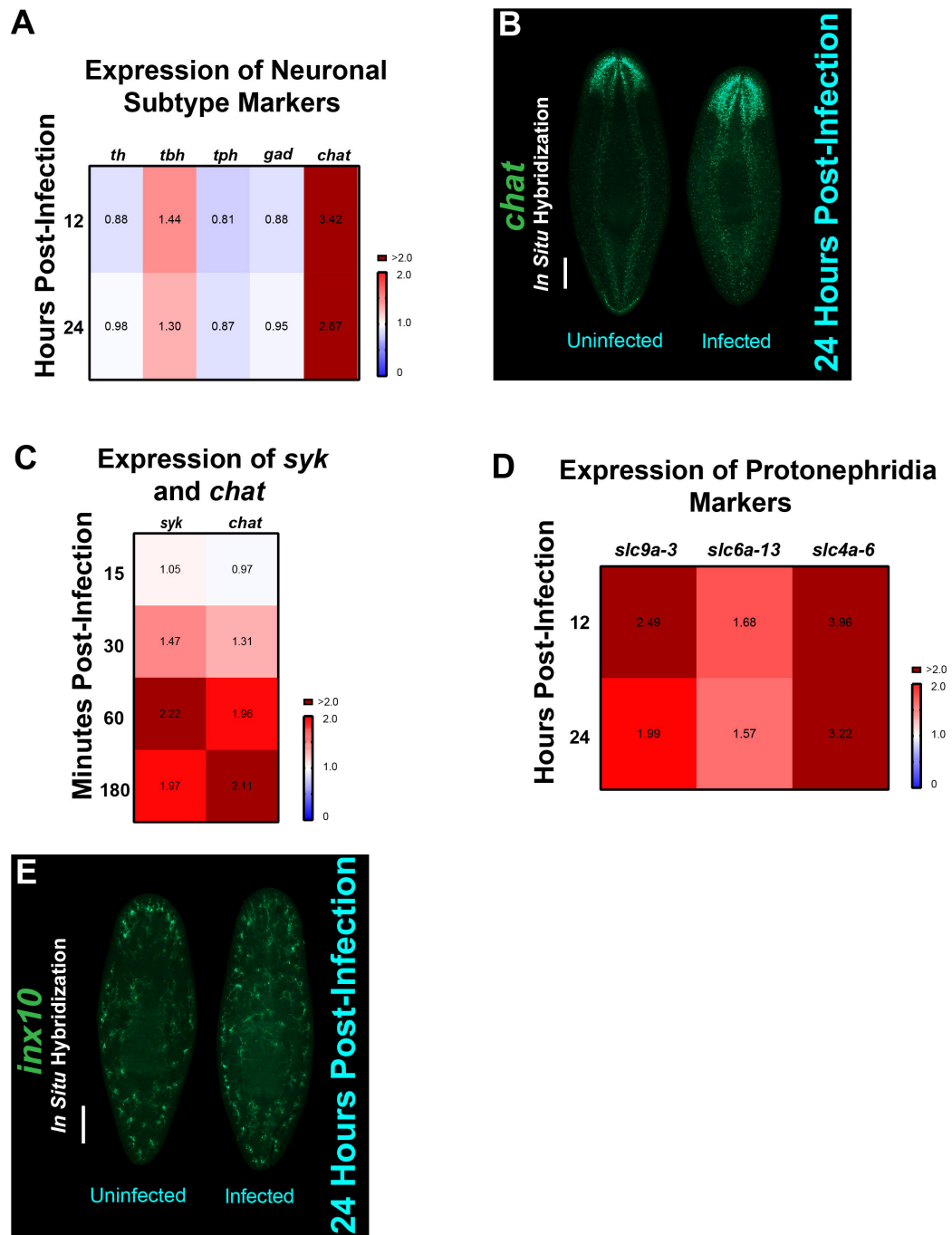
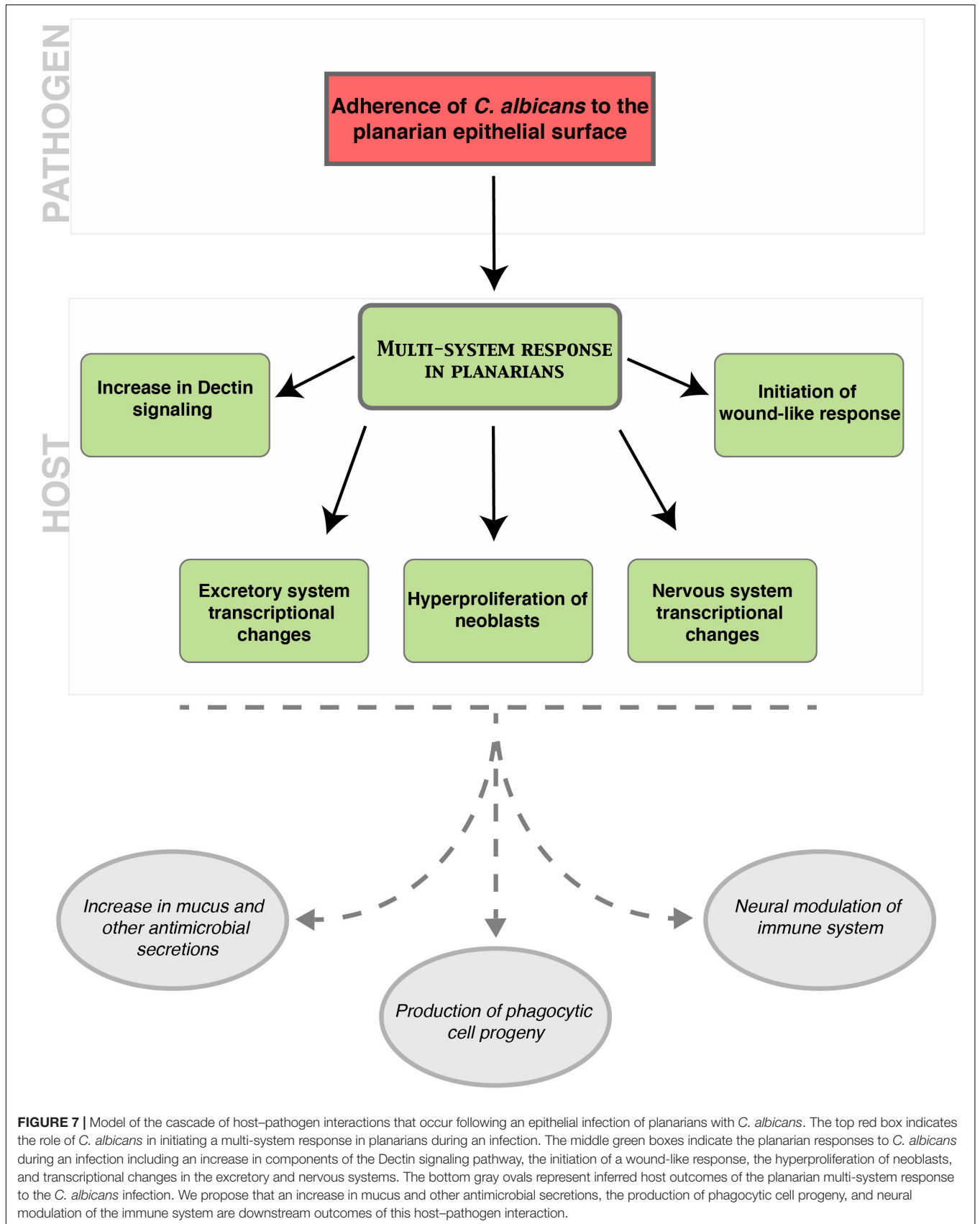


FIGURE 6 | Neurons, protonephridia, and specific mesenchymal neoblast markers are upregulated in planarians during infection with *C. albicans*. **(A)** Expression of five different neuron subtypes. Gene expression levels throughout the course of the *C. albicans* infection are represented in the heat map, where the color scale depicts red as upregulation and blue as downregulation; burgundy is upregulation greater than twofold. Gene expression is represented by fold change normalized to an uninfected control. **(B)** Fluorescent *in situ* hybridization showing expression of *chat* in an uninfected and 24-h infected planarian. Scale bar is 200 μ m. Images are representative of eight animals for at least two biological and technical replicates. **(C)** Gene expression levels of *syk* and *chat* throughout the course of the *C. albicans* infection (15–180 min). Expression levels are represented in a heat map, where the color scale depicts red as upregulation and blue as downregulation; burgundy is upregulation greater than twofold. Gene expression is represented by fold change normalized to an uninfected control. Gene expression values represent triplicate samples for at least two biological and technical replicates. **(D)** Expression of protonephridia structure markers: *slc9a-3* (collecting ducts), *slc4a-6* (distal tubules), and *slc6a-13* (proximal tubules). Gene expression levels throughout the course of the *C. albicans* infection are represented in the heat map, where the color scale depicts red as upregulation and blue as downregulation; burgundy is upregulation greater than twofold. Gene expression is represented by fold change normalized to an uninfected control. **(E)** Fluorescent *in situ* hybridization showing expression of *inx10* in an uninfected and 24-h infected animal. Scale bar is 200 μ m. Images are representative of eight animals for at least two biological and technical replicates.



Our results reveal that part of the host response to *C. albicans* epithelial infection involves a stereotypical pattern of neoblast division. Two systemic peaks of neoblast division occur at six and 24 hpi without visible signs of host tissue damage. This is intriguing because physiological increases in neoblast division generally occur via metabolic inputs such as nutrient availability through feeding or in response to tissue injury (Saló and Baguña, 1984; Wenemoser and Reddien, 2010; Peiris et al., 2012). The metabolic-induced neoblast hyperproliferation is systemic and tends to peak around 6–12 h post-feeding to gradually return to pre-feeding levels by 48 h (Baguña, 1976; Kang and Sánchez Alvarado, 2009). The amputation-induced neoblast division takes place as biphasic peaks that occur first systemically at 6 h post-amputation and then localized near the injury site between 48–72 h following wounding (Wenemoser and Reddien, 2010). Our findings suggest that similar to amputation, fungal infection triggers neoblast proliferation by 6 hpi and it is preceded by ERK phosphorylation and the overexpression of the early wound response gene *egr2* (Wenemoser and Reddien, 2010; Owlarn et al., 2017). However, the neoblast response to *C. albicans* infection does not involve an increase in the expression of *runt1*, which is important for regeneration, and is not triggered by major tissue damage as observed by amputation or the resulting distention of the intestine that occurs after feeding. Furthermore, the second mitotic peak observed after fungal infection is systemic and occurs roughly 18 h after the initial peak. Another striking difference with the regeneration response is that cell death does not precede the neoblast increase in proliferation during the early stages of infection (**Supplementary Figure 3**). Therefore, the mitotic response to fungal infection differs in time and location with respect to other stimuli such as feeding and amputation. We speculate that *C. albicans* infection activates an infection-specific neoblast proliferative response.

The neoblast hyper-proliferative response is preceded by the adherence of *C. albicans* to the planarian epithelial surface. This response is dependent on the *C. albicans* transcription factor Bcr1, which is a major regulator of adherence, and its downstream GPI-anchored protein Als3, which is an important adhesin. Although the precise molecular mechanisms leading to hyper-proliferation in planarians in response to infection with *C. albicans* are unclear, it seems likely that the ability of *C. albicans* to adhere to the planarian epithelial surface is a critical factor in inducing this response. Given that Bcr1 controls the expression of numerous genes encoding cell wall proteins, and is a major regulator of biofilm formation (Nobile and Mitchell, 2005; Nobile et al., 2006, 2012), it seems likely that the ability to colonize and form biofilms on the planarian epithelial surface are important fungal processes in initiating this hyper-proliferative host response. Als3 is also required for biofilm formation in *C. albicans* and is a major adhesin expressed on the surface of hyphal cells. Thus, the ability to form adhesive hyphae that can actively penetrate host epithelial cells is another factor that likely mediates this host response (Wachtler et al., 2011). Interestingly, Als3 is known to bind to mammalian host ligands, such as *E*-cadherin on epithelial cells and *N*-cadherin on endothelial cells (Phan et al., 2005, 2007), which induces

engulfment of fungal cells into the mammalian host via a clathrin-dependent mechanism. Given the importance of Als3 in triggering hyper-proliferation in planarians, it is possible that the process of host cell engulfment of *C. albicans* cells is also involved in initiating this host response. Taken together, it seems likely that both invasion mechanisms of induced endocytosis as well as active penetration of *C. albicans* cells are complementary mechanisms that induce hyper-proliferation of the planarian host.

Adherence of *C. albicans* cells to the planarian epithelial surface is followed by a generalized overexpression of host genes associated with the Dectin signaling pathway. In our previous work (Maciel et al., 2019), we also observed an overexpression of components of the Dectin signaling pathway (*syk* and *tak*) at later timepoints of the infection, suggesting that there is a consistent innate immune response in planarians during fungal infection. A key component of the Dectin signaling pathway is the adaptor protein SYK, and our results show a persistent overexpression of the *syk* gene throughout infection with *C. albicans*. Unexpectedly, functional disruption of *syk* by RNAi resulted in a slight increase in neoblast proliferation upon *C. albicans* infection. It remains unclear why this apparent increase in neoblast proliferation is accompanied by a delayed clearance of the infection. It is possible that this is due to redundancy with other pathways or to an aberrant neoblast response to infection. Nonetheless, these findings suggest that *syk* is required for planarians to clear the *C. albicans* infection in a timely manner. Overall, although Dectin signaling is activated in planarians upon fungal infection, the canonical Dectin-1 C-type lectin pattern-recognition receptor has not yet been identified in planarians and planarian species are known to have a number of C-type lectin-like proteins (Shagin et al., 2002; Gao et al., 2017). Thus, additional experiments will be needed to identify potential pattern-recognition receptors in planarians, and to understand the molecular cascade and the evolutionary conservation of the Dectin signaling pathway in planarians with other animals, including humans and other vertebrates.

As part of the host response to *C. albicans* infection, we observed a differential expression in planarian markers of neoblast subpopulations. This finding suggests that not all neoblasts are engaged in the response to fungal infection and opens up the possibility of an infection-specific neoblast response. Recent work classified neoblast subpopulations based on the content of the marker *piwi-1* (Zeng et al., 2018). This study found that neoblasts with high *piwi-1* content (*piwi-1^{high}*) include the clonogenic neoblasts (cNeoblasts) that together are key players in the early regenerative response (Zeng et al., 2018). However, we found that the expression of markers for neoblast subpopulations with the highest content of *piwi-1* (e.g., NB1, NB2, and NB3) remained relatively low or did not change relative to the uninfected group in the initial 48 hpi. Instead, there was a dramatic increase in the expression of markers for neoblasts with reduced levels of *piwi-1* (i.e., NB4, NB5, NB7, NB9, and NB11) upon *C. albicans* infection. From these neoblast subclasses NB9, NB11, and NB4 displayed the highest expression levels, greater than eightfold

in the initial 48 hpi. These three neoblast subpopulations contain less than 5% of *piwi-1* positive cells (Zeng et al., 2018). This finding raises the possibility that the active cycling of neoblasts with low *piwi-1* content could be responsible for the two mitotic peaks we observed during infection with *C. albicans*. We propose that *C. albicans* infection elicits a heterogeneous neoblast response that is distinct from that observed during regeneration.

Our findings indicate that the host response to *C. albicans* infection involves transcriptional changes in distinct differentiated planarian tissues. The upregulation in the expression of genes associated with the excretory system is detected as early as 12 hpi. The increased expression of genes within the excretory system may lead to an enhanced secretion of mucus, which contains antimicrobial components to aid in the elimination of the pathogen. The mucus barrier in planarians contains an extensive array of antimicrobial peptides, zymogens, and proteases that aid in the innate immune response to infection (Bocchini et al., 2012). Likewise, the dramatic increase in the expression of the marker of cholinergic neurons (*chat*) in the initial 24 hpi, suggests that this neuronal type may be important in the innate immune response to *C. albicans* infection. This is consistent with the idea that certain neuronal groups can act as immunocompetent cells, which is an ancient function conserved between pre-bilaterians and mammals (Godinho-Silva et al., 2019; Klimovich et al., 2020). Indeed, murine nociceptive neurons are critical for the innate immune response to cutaneous infection with *C. albicans* (Kashem et al., 2015). Together, the increase in expression of markers of the neural and the excretory systems in planarians suggests the existence of long-range organismal communication that is likely needed to orchestrate defense against invading pathogens. It is tempting to speculate that the adherence of *C. albicans* cells to the planarian epithelial surface may trigger neural cues that activate the secretion of mucus with antimicrobial properties and the innate immune response through the Dectin signaling pathway. Future experiments will address the precise interplay between neoblasts, differentiated tissues and the molecular cascade orchestrated by the planarian innate immune system to defend against invading pathogens (Figure 7).

DATA AVAILABILITY STATEMENT

The original contributions generated for this study are included in the article/Supplementary Material, further inquiries can be directed to the corresponding author/s.

AUTHOR CONTRIBUTIONS

EM, AV, BZ, CN, and NO conceived, designed, and interpreted the experiments. EM, AV, and BZ performed all the experiments and acquired and analyzed the data. EM, AV, BZ, CN, and NO wrote the manuscript. All authors read the manuscript, provided comments, and approved the final version.

FUNDING

This work was supported by the National Institutes of Health (NIH), National Institute of Allergy and Infectious Diseases (NIAID), and the National Institute of General Medical Sciences (NIGMS) awards R21AI125801 and R35GM124594, respectively to CN; by a Pew Biomedical Scholar Award from the Pew Charitable Trusts to CN; and by the Kamangar family in the form of an endowed chair to CN. This work was also supported by the University of California Cancer Research Coordinating Committee award CRR-18-525108 and the NIGMS award R01GM132753 to NO. AV was supported by diversity supplement fellowship R21AI125801-02S1 to parent grant R21AI125801. EM was supported by the National Science Foundation (NSF) graduate fellowship award 1744620. The funders had no role in the study design, data collection and interpretation, or the decision to submit the work for publication.

ACKNOWLEDGMENTS

We thank Edelweiss Pfister for lab management and planarian maintenance in the Oviedo lab, and Gurbinder Singh for technical assistance in the Nobile lab. We thank all members of the Nobile and Oviedo labs for insightful discussions and comments on the manuscript. We thank Dr. K. Bartscherer for kindly providing the pERK antibody. We also thank Dr. Bernhard Hube for the gift of the *C. albicans sap1/sap2/sap3* and *sap4/sap5/sap6* triple mutant strains. The anti-actin antibody was obtained from the Developmental Studies Hybridoma Bank, created by the National Institutes of Health (NIH), National Institute of Child Health and Human Development (NICHD), and maintained at the University of Iowa, Department of Biology.

SUPPLEMENTARY MATERIAL

The Supplementary Material for this article can be found online at: <https://www.frontiersin.org/articles/10.3389/fmicb.2020.629526/full#supplementary-material>

Supplementary Figure 1 | Orientation and basic anatomy of the planarian body. **(A)** Demonstrates the orientation the planarians in the whole-mount images. **(B)** Depiction of a transverse cross section of a planarian in the orientation found in the images throughout the figures. **(C)** Depiction of the digestive system, nervous system, and protonephridia of planarians.

Supplementary Figure 2 | Cross section images of the planarian body during early infection with *C. albicans*. Individual transverse cross section images are displayed from the dorsal side of the planarian body showing staining with the DAPI nuclear marker (white signal), anti-*Candida* antibody (red signal), and merged images, at 1, 3, and 6 h post-infection. Yellow triangles indicate notable *C. albicans* aggregates.

Supplementary Figure 3 | Cell death occurring during the early stages of infection with *C. albicans*. **(A)** TUNEL staining (red foci) was performed in uninfected planarians to compare animals infected at 2 and 4 h post-infection using 25 million cells/mL of *C. albicans*. **(B)** Levels of TUNEL+ cells in the planarian tissue 2 and 4 h post-infection normalized to an uninfected control. Cell death experiments consisted of two biological replicates using four animals each. All graphs represent mean \pm SEM. Scale bar is 200 μ m.

REFERENCES

- Baguña, J. (1976). Mitosis in the intact and regenerating planarian *Dugesia mediterranea* n.sp. I. mitotic studies during growth, feeding and starvation. *J. Exp. Zool.* 195, 53–64. doi: 10.1002/jez.1401950106
- Bergeron, A. C., Barker, S. E., Brothers, K. M., Prasad, B. C., and Wheeler, R. T. (2017). Polyclonal anti-Candida antibody improves phagocytosis and overall outcome in zebrafish model of disseminated candidiasis. *Dev. Comp. Immunol.* 68, 69–78. doi: 10.1016/j.dci.2016.11.017
- Bocchinfuso, D. G., Taylor, P., Ross, E., Ignatchenko, A., Ignatchenko, V., Kislinger, T., et al. (2012). Proteomic profiling of the planarian *Schmidtea mediterranea* and its mucous reveals similarities with human secretions and those predicted for parasitic flatworms. *Mol. Cell. Proteom.* 11, 681–691. doi: 10.1074/mcp.m112.019026
- Braun, B. R., and Johnson, A. D. (1997). Control of filament formation in *Candida albicans* by the transcriptional repressor TUP1. *Science* 277, 105–109. doi: 10.1126/science.277.5322.105
- Brunke, S., and Hube, B. (2014). Adaptive prediction as a strategy in microbial infections. *PLoS Pathog* 10:e1004356. doi: 10.1371/journal.ppat.1004356
- Chamilos, G., Lewis, R. E., Albert, N., and Kontoyiannis, D. P. (2007). Paradoxical effect of *Echinocandins* across *Candida* species in vitro: evidence for echinocandin-specific and candida species-related differences. *Antimicrob Agents Chemother* 51, 2257–2259. doi: 10.1128/aac.00095-07
- Espinosa, V., and Rivera, A. (2016). First line of defense: innate cell-mediated control of pulmonary *Aspergillosis*. *Front. Microbiol.* 7:272. doi: 10.3389/fmicb.2016.00272
- Felk, A., Kretschmar, M., Albrecht, A., Schaller, M., Beinhauer, S., Nichterlein, T., et al. (2002). *Candida albicans* hyphal formation and the expression of the Efg1-regulated proteinases Sap4 to Sap6 are required for the invasion of parenchymal organs. *Infect. Immun.* 70, 3689–3700. doi: 10.1128/iai.70.7.3689-3700.2002
- Filler, S. G. (2013). Can host receptors for fungi be targeted for treatment of fungal infections? *Trends Microbiol.* 21, 389–396. doi: 10.1016/j.tim.2013.05.006
- Filler, S. G., Swerdloff, J. N., Hobbs, C., and Luckett, P. M. (1995). Penetration and damage of endothelial cells by *Candida albicans*. *Infect. Immun.* 63, 976–983. doi: 10.1128/iai.63.3.976-983.1995
- Gao, L., Han, Y., Deng, H., Hu, W., Zhen, H., Li, N., et al. (2017). The role of a novel C-type lectin-like protein from planarian in innate immunity and regeneration. *Dev. Comp. Immunol.* 67, 413–426. doi: 10.1016/j.dci.2016.08.010
- Glittenberg, M. T., Silas, S., MacCallum, D. M., Gow, N. A., and Ligoxygakis, P. (2011). Wild-type *Drosophila melanogaster* as an alternative model system for investigating the pathogenicity of *Candida albicans*. *Dis. Models Mechan.* 4, 504–514. doi: 10.1242/dmm.006619
- Godinho-Silva, C., Cardoso, F., and Veiga-Fernandes, H. (2019). Neuro-Immune cell units: a new paradigm in physiology. *Annu. Rev. Immunol.* 37, 19–46. doi: 10.1146/annurev-immunol-042718-041812
- Gratacap, R. L., Scherer, A. K., Seman, B. G., and Wheeler, R. T. (2017). Control of mucosal candidiasis in the zebrafish swimbladder depends on neutrophils that block filament invasion and drive extracellular trap production. *Infect. Immun.* 85:e00276-17.
- Homann, O. R., Dea, J., Noble, S. M., and Johnson, A. D. (2009). A phenotypic profile of the *Candida albicans* regulatory network. *PLoS Genet.* 5:e1000783. doi: 10.1371/journal.pgen.1000783
- Hoyer, L. L., and Cota, E. (2016). *Candida albicans* Agglutinin-Like Sequence (Als) family vignettes: a review of als protein structure and function. *Front. Microbiol.* 7:280. doi: 10.3389/fmicb.2016.00280
- Kang, H., and Sánchez Alvarado, A. (2009). Flow cytometry methods for the study of cell-cycle parameters of planarian stem cells. *Dev. Dynam.* 238, 1111–1117. doi: 10.1002/dvdy.21928
- Kashem, S. W., Riedl, M. S., Yao, C., Honda, C. N., Vulchanova, L., and Kaplan, D. H. (2015). Nociceptive sensory fibers drive interleukin-23 Production from CD301b+ dermal dendritic cells and drive protective cutaneous immunity. *Immunity* 43, 515–526. doi: 10.1016/j.immuni.2015.08.016
- King, R. S., and Newmark, P. A. (2013). In situ hybridization protocol for enhanced detection of gene expression in the planarian *Schmidtea mediterranea*. *BMC Dev. Biol.* 13:8. doi: 10.1186/1471-213X-13-8
- Klimovich, A., Giacomello, S., Bjorklund, A., Faure, L., Kaucka, M., Giez, C., et al. (2020). Prototypical pacemaker neurons interact with the resident microbiota. *Proc. Natl. Acad. Sci. U S A.* 117, 17854–17863. doi: 10.1073/pnas.1920469117
- Maciel, E. I., Jiang, C., Barghouth, P. G., Nobile, C. J., and Oviedo, N. J. (2019). The planarian *Schmidtea mediterranea* is a new model to study host-pathogen interactions during fungal infections. *Dev. Comp. Immunol.* 93, 18–27. doi: 10.1016/j.dci.2018.12.005
- Mallick, E. M., Bergeron, A. C., Jones, S. K. Jr., Newman, Z. R., Brothers, K. M., et al. (2016). Phenotypic plasticity regulates *Candida albicans* interactions and virulence in the vertebrate host. *Front. Microbiol.* 7:780. doi: 10.3389/fmicb.2016.00780
- Mayer, F. L., Wilson, D., and Hube, B. (2013). *Candida albicans* pathogenicity mechanisms. *Virulence* 4, 119–128.
- Megías, J., Martínez, A., Yáñez, A., Goodridge, H. S., Gozalbo, D., and Gil, L. M. (2016). TLR2, TLR4 and Dectin-1 signalling in hematopoietic stem and progenitor cells determines the antifungal phenotype of the macrophages they produce. *Microbes Infect.* 18, 354–363. doi: 10.1016/j.micinf.2016.01.005
- Megías, J., Yáñez, A., Moriano, S., O'Connor, J. E., Gozalbo, D., and Gil, M. L. (2012). Direct Toll-like receptor-mediated stimulation of hematopoietic stem and progenitor cells occurs in vivo and promotes differentiation toward macrophages. *Stem Cells* 30, 1486–1495. doi: 10.1002/stem.1110
- Mitchell, A. P. (1998). Dimorphism and virulence in *Candida albicans*. *Curr. Opin. Microbiol.* 1, 687–692. doi: 10.1016/s1369-5274(98)80116-1
- Moreno-Ruiz, E., Galan-Diez, M., Zhu, W., Fernandez-Ruiz, E., d'Enfert, C., Filler, S. G., et al. (2009). *Candida albicans* internalization by host cells is mediated by a clathrin-dependent mechanism. *Cell Microbiol.* 11, 1179–1189. doi: 10.1111/j.1462-5822.2009.01319.x
- Mylonakis, E. (2008). *Galleria mellonella* and the study of fungal pathogenesis: making the case for another genetically tractable model host. *Mycopathologia* 165, 1–3. doi: 10.1007/s11046-007-9082-z
- Mylonakis, E., Casadevall, A., and Ausubel, F. M. (2007). Exploiting amoeboid and non-vertebrate animal model systems to study the virulence of human pathogenic fungi. *PLoS Pathog* 3:e101. doi: 10.1371/journal.ppat.0030101
- Naglik, J. R., Challacombe, S. J., and Hube, B. (2003). *Candida albicans* secreted aspartyl proteinases in virulence and pathogenesis. *Microbiol. Mol. Biol. Rev.* 67, 400–428. doi: 10.1128/mmr.67.3.400-428.2003
- Nobile, C. J., Andes, D. R., Nett, J. E., Smith, F. J., Yue, F., Phan, Q.-T. T., et al. (2006). Critical role of Bcr1-dependent adhesins in *C. albicans* biofilm formation in vitro and in vivo. *PLoS Pathogens* 2:e63. doi: 10.1371/journal.ppat.0020063
- Nobile, C. J., Fox, E. P., Nett, J. E., Sorrells, T. R., Mitrovich, Q. M., Hernday, A. D., et al. (2012). A recently evolved transcriptional network controls biofilm development in *Candida albicans*. *Cell* 148, 126–138. doi: 10.1016/j.cell.2011.10.048
- Nobile, C. J., and Johnson, A. D. (2015). *Candida albicans* biofilms and human disease. *Annu. Rev. Microbiol.* 69, 71–92.
- Nobile, C. J., and Mitchell, A. P. (2005). Regulation of cell-surface genes and biofilm formation by the *C. albicans* transcription factor Bcr1p. *Curr. Biol.* 15, 1150–1155. doi: 10.1016/j.cub.2005.05.047
- Nobile, C. J., Schneider, H. A., Nett, J. E., Sheppard, D. C., Filler, S. G., Andes, D. R., et al. (2008). Complementary adhesion function in *C. albicans* biofilm formation. *Curr. Biol.* 18, 1017–1024. doi: 10.1016/j.cub.2008.06.034
- Oviedo, N. J., and Levin, M. (2007). smedinx-11 is a planarian stem cell gap junction gene required for regeneration and homeostasis. *Development* 134, 3121–3131. doi: 10.1242/dev.006635
- Oviedo, N. J., Nicolas, C., Adams, D. S., and Levin, M. (2008a). Gene knockdown in planarians using RNAi interference. *Cold Spring Harb Protocols* 3, 902–906.
- Oviedo, N. J., Nicolas, C. L., Adams, D. S., and Levin, M. (2008b). Establishing and maintaining a colony of planarians. *CSH Protocols* 2008:pdb.prot5053. doi: 10.1101/pdb.prot5053
- Owllarn, S., Klenner, F., Schmidt, D., Rabert, F., Tomasso, A., Reuter, H., et al. (2017). Generic wound signals initiate regeneration in missing-tissue contexts. *Nat. Commun.* 8:2282.
- Pearson, B. J., Eisenhoffer, G. T., Gurley, K. A., Rink, J. C., Miller, D. E., and Sánchez Alvarado, A. (2009). Formaldehyde-based whole-mount in situ hybridization method for planarians. *Dev. Dynam.* 238, 443–450. doi: 10.1002/dvdy.21849
- Peiris, T. H., Hoyer, K. K., and Oviedo, N. J. (2014). Innate immune system and tissue regeneration in planarians: an area ripe for exploration. *Semin. Immunol.* 26, 295–302. doi: 10.1016/j.smim.2014.06.005
- Peiris, T. H., Weckerle, F., Ozamoto, E., Ramirez, D., Davidian, D., Garcia-Ojeda, M. E., et al. (2012). TOR signaling regulates planarian stem cells and controls

- localized and organismal growth. *J. Cell Sci.* 125, 1657–1665. doi: 10.1242/jcs.104711
- Pellon, A., Sadeghi Nasab, S. D., and Moyes, D. L. (2020). New Insights in *Candida albicans* innate immunity at the mucosa: Toxins, Epithelium, metabolism, and beyond. *Front. Cell Infect. Microbiol.* 10:81. doi: 10.3389/fcimb.2020.00081
- Peterson, N. D., and Pukkila-Worley, R. (2018). Caenorhabditis elegans in high-throughput screens for anti-infective compounds. *Curr. Opin. Immunol.* 54, 59–65. doi: 10.1016/j.coi.2018.06.003
- Phan, Q. T., Fratti, R. A., Prasadarao, N. V., Edwards, J. E. Jr., and Filler, S. G. (2005). N-cadherin mediates endocytosis of *Candida albicans* by endothelial cells. *J. Biol. Chem.* 280, 10455–10461. doi: 10.1074/jbc.M412592200
- Phan, Q. T., Myers, C. L., Fu, Y., Sheppard, D. C., Yeaman, M. R., Welch, W. H., et al. (2007). Als3 is a *Candida albicans* invasin that binds to cadherins and induces endocytosis by host cells. *PLoS Biol.* 5:e64. doi: 10.1371/journal.pbio.0050064
- Pukkila-Worley, R., Holson, E., Wagner, F., and Mylonakis, E. (2009). Antifungal drug discovery through the study of invertebrate model hosts. *Curr. Med. Chem.* 16, 1588–1595. doi: 10.2174/092986709788186237
- Rink, J. C., Vu, H. T., and Sanchez Alvarado, A. (2011). The maintenance and regeneration of the planarian excretory system are regulated by EGFR signaling. *Development* 138, 3769–3780. doi: 10.1242/dev.066852
- Ross, K. G., Currie, K. W., Pearson, B. J., and Zayas, R. M. (2017). Nervous system development and regeneration in freshwater planarians. *Wiley Interdiscipl. Rev. Dev. Biol.* 6:e266. doi: 10.1002/wdev.266
- Saló, E., and Baguña, J. (1984). Regeneration and pattern formation in planarians. I. The pattern of mitosis in anterior and posterior regeneration in *Dugesia* (G) tigrina, and a new proposal for blastema formation. *J. Embryol. Exp. Morphol.* 83, 63–80.
- Sandmann, T., Vogg, M. C., Owlarn, S., Boutros, M., and Bartscherer, K. (2011). The head-regeneration transcriptome of the planarian *Schmidtea mediterranea*. *Genome Biol.* 12, R76.
- Saville, S. P., Lazzell, A. L., Monteagudo, C., and Lopez-Ribot, J. L. (2003). Engineered control of cell morphology in vivo reveals distinct roles for yeast and filamentous forms of *Candida albicans* during infection. *Eukaryot Cell* 2, 1053–1060. doi: 10.1128/ec.2.5.1053-1060.2003
- Schneider, C. A., Rasband, W. S., and Eliceiri, K. W. (2012). NIH Image to ImageJ: 25 years of image analysis. *Nat. Methods* 9, 671–675. doi: 10.1038/nmeth.2089
- Segal, E., and Frenkel, M. (2018). Experimental in vivo models of candidiasis. *J. Fungi (Basel)* 4:21. doi: 10.3390/jof4010021
- Shagin, D. A., Barsova, E. V., Bogdanova, E., Britanova, O. V., Gurskaya, N., Lukyanov, K. A., et al. (2002). Identification and characterization of a new family of C-type lectin-like genes from planaria *Girardia tigrina*. *Glycobiology* 12, 463–472. doi: 10.1093/glycob/cwf056
- Sun, J. N., Solis, N. V., Phan, Q. T., Bajwa, J. S., Kashleva, H., Thompson, A., et al. (2010). Host cell invasion and virulence mediated by *Candida albicans* Ssa1. *PLoS Pathog* 6:e1001181. doi: 10.1371/journal.ppat.1001181
- Valle Arevalo, A., and Nobile, C. J. (2020). Interactions of microorganisms with host mucins: a focus on *Candida albicans*. *FEMS Microbiol. Rev.* 44, 645–654. doi: 10.1093/femsre/ruaa027
- Wachtler, B., Citiulo, F., Jablonowski, N., Forster, S., Dalle, F., Schaller, M., et al. (2012). *Candida albicans*-epithelial interactions: dissecting the roles of active penetration, induced endocytosis and host factors on the infection process. *PLoS One* 7:e36952. doi: 10.1371/journal.pone.0036952
- Wachtler, B., Wilson, D., Haedicke, K., Dalle, F., and Hube, B. (2011). From attachment to damage: defined genes of *Candida albicans* mediate adhesion, invasion and damage during interaction with oral epithelial cells. *PLoS One* 6:e17046. doi: 10.1371/journal.pone.0017046
- Wagener, M., Hoving, J. C., Ndlovu, H., and Marakalala, M. J. (2018). Dectin-1-Syk-CARD9 signaling pathway in TB immunity. *Front. Immunol.* 9:225. doi: 10.3389/fimmu.2018.00225
- Wagner, D. E., Wang, I. E., and Reddien, P. W. (2011). Clonogenic neoblasts are pluripotent adult stem cells that underlie planarian regeneration. *Science* 332, 811–816. doi: 10.1126/science.1203983
- Wenemoser, D., Lapan, S. W., Wilkinson, A. W., Bell, G. W., and Reddien, P. W. (2012). A molecular wound response program associated with regeneration initiation in planarians. *Genes Dev.* 26, 988–1002. doi: 10.1101/gad.187377.112
- Wenemoser, D., and Reddien, P. W. (2010). Planarian regeneration involves distinct stem cell responses to wounds and tissue absence. *Dev. Biol.* 344, 979–991. doi: 10.1016/j.ydbio.2010.06.017
- Wilson, D., Naglik, J. R., and Hube, B. (2016). The missing link between candida albicans hyphal morphogenesis and host cell damage. *PLoS Pathog* 12:e1005867. doi: 10.1371/journal.ppat.1005867
- Wurtzel, O., Cote, L. E., Poirier, A., Satija, R., Regev, A., and Reddien, P. W. (2015). A Generic and Cell-Type-Specific wound response precedes regeneration in planarians. *Dev. Cell* 35, 632–645. doi: 10.1016/j.devcel.2015.11.004
- Yáñez, A., Megias, J., O'Connor, J.-E., Gozalbo, D., and Gil, L. M. (2011). *Candida albicans* induces selective development of macrophages and monocyte derived dendritic cells by a TLR2 dependent signalling. *PLoS One* 6:e24761. doi: 10.1371/journal.pone.0024761
- Yáñez, A., Murciano, C., O'Connor, J.-E., Gozalbo, D., and Gil, L. M. (2009). *Candida albicans* triggers proliferation and differentiation of hematopoietic stem and progenitor cells by a MyD88-dependent signaling. *Microbes Infect.* 11, 531–535. doi: 10.1016/j.micinf.2009.01.011
- Yang, R., Liu, Y., Kelk, P., Qu, C., Akiyama, K., Chen, C., et al. (2012). A subset of IL-17+ mesenchymal stem cells possesses anti-*Candida albicans* effect. *Cell Res.* 23, 107–121. doi: 10.1038/cr.2012.179
- Zeng, A., Li, H., Guo, L., Gao, X., McKinney, S., Wang, Y., et al. (2018). Prospectively isolated tetraspanin + neoblasts are adult pluripotent stem cells underlying planaria regeneration. *Cell* 173, 1593–1608.e20.
- Ziman, B., Karabinis, P., Barghouth, P., and Oviedo, N. J. (2020). Sirtuin-1 regulates organismal growth by altering feeding behavior and intestinal morphology in planarians. *J. Cell Sci.* 133:jcs239467. doi: 10.1242/jcs.239467

Conflict of Interest: CN is a cofounder of BioSynthesis, Inc., a company developing inhibitors and diagnostics of biofilm infections.

The remaining authors declare that the research was conducted in the absence of any commercial or financial relationships that could be construed as a potential conflict of interest.

Copyright © 2021 Maciel, Valle Arevalo, Ziman, Nobile and Oviedo. This is an open-access article distributed under the terms of the Creative Commons Attribution License (CC BY). The use, distribution or reproduction in other forums is permitted, provided the original author(s) and the copyright owner(s) are credited and that the original publication in this journal is cited, in accordance with accepted academic practice. No use, distribution or reproduction is permitted which does not comply with these terms.